Title

Human intelectin-2 (ITLN2) is selectively expressed by secretory Paneth cells

Journal

The FASEB Journal, 36(3)

ISSN

0892-6638

Authors

Nonnecke, Eric B

Castillo, Patricia A

Johansson, Malin EV

et al.

Publication Date

2022-03-01

DOI

10.1096/fj.202101870r

Peer reviewed

Received: 6 December 2021 | Revised: 20 January 2022 | Accepted: 26 January 2022

DOI: 10.1096/fj.202101870R

THE FASEB JOURNAL

RESEARCH ARTICLE

Human intelectin-2 (ITLN2) is selectively expressed by secretory Paneth cells

Eric B. Nonnecke[1] | **Patricia A. Castillo**[1] | **Malin E. V. Johansson**[2] | **Edward J. Hollox**[3] | **Bo Shen**[4] | **Bo Lönnerdal**[5] | **Charles L. Bevins**[1]

[1]Department of Microbiology and Immunology, School of Medicine, University of California, Davis, Davis, California, USA

[2]Department of Medical Biochemistry and Cell Biology, Institute of Biomedicine, University of Gothenburg, Gothenburg, Sweden

[3]Department of Genetics and Genome Biology, University of Leicester, Leicester, UK

[4]Department of Gastroenterology, Hepatology and Nutrition, Digestive Diseases and Surgery Institute, Cleveland Clinic, Cleveland, Ohio, USA

[5]Department of Nutrition, University of California, Davis, Davis, California, USA

Correspondence
Eric B. Nonnecke and Charles L. Bevins, Department of Microbiology and Immunology, School of Medicine, University of California, Davis, Davis, CA 95616, USA.
Email: ebnonnecke@ucdavis.edu and clbevins@ucdavis.edu

Present address
Bo Shen, Department of Surgery, Columbia University Vagelos College of Physicians and Surgeons, 10032, New York, New York, USA

Patricia A. Castillo, Elanco Animal Health, 50501, Fort Dodge, Iowa, USA

Funding information
National Institutes of Health, Grant/Award Number: U01AI125926 and R37AI32738

Abstract

Intelectins (intestinal lectins) are highly conserved across chordate evolution and have been implicated in various human diseases, including Crohn's disease (CD). The human genome encodes two intelectin genes, intelectin-1 (*ITLN1*) and intelectin-2 (*ITLN2*). Other than its high sequence similarity with ITLN1, little is known about ITLN2. To address this void in knowledge, we report that ITLN2 exhibits discrete, yet notable differences from ITLN1 in primary structure, including a unique amino terminus, as well as changes in amino acid residues associated with the glycan-binding activity of ITLN1. We identified that ITLN2 is a highly abundant Paneth cell-specific product, which localizes to secretory granules, and is expressed as a multimeric protein in the small intestine. In surgical specimens of ileal CD, *ITLN2* mRNA levels were reduced approximately five-fold compared to control specimens. The ileal expression of *ITLN2* was unaffected by previously reported disease-associated variants in *ITLN2* and CD-associated variants in neighboring *ITLN1* as well as *NOD2* and *ATG16L1*. *ITLN2* mRNA expression was undetectable in control colon tissue; however, in both ulcerative colitis (UC) and colonic CD, metaplastic Paneth cells were found to express ITLN2. Together, the data reported establish the groundwork for understanding ITLN2 function(s) in the intestine, including its possible role in CD.

KEYWORDS

alpha-defensin, Crohn's disease, innate immunity, intelectin, lectin, metaplasia, omentin, Paneth cell, small intestine, ulcerative colitis

1 | INTRODUCTION

Intelectins are highly conserved across chordate evolution and are abundantly expressed at mucosal surfaces, including the small intestine and colon of mammals.[1] The human genome encodes two intelectin genes (*ITLN1* and *ITLN2*) tandemly arranged on chromosome 1q23.3. Variants within human *ITLN1*, which encodes a lectin that targets acyclic vicinal (1,2)-diol moieties present on microbial but not mammalian glycans, have been identified by genome-wide association studies (GWAS) as risk loci for Crohn's disease (CD); however, the mechanisms underlying this association remain to be elucidated.[2–9] ITLN1, sometimes referred to as omentin, is expressed in several tissues, including goblet cells of the small and large intestine, as well as lung, visceral adipose, and serum.[9–14] In contrast, the expression of ITLN2 appears to be more restricted to intestinal tissues and is less well characterized.[11,14] Clarifying the cellular source(s) of human ITLNs remains a pressing question.

Mouse Itln1, a functional ortholog of human ITLN1, is expressed in small intestinal Paneth cells—specialized secretory epithelial cells located in the crypts of Lieberkühn.[2,15] In both mice and humans, Paneth cells express an array of abundant and luminally secreted antimicrobial effectors, including α-defensins, lysozyme, and Reg family proteins, which mediate host-microbe interactions.[16,17] In addition, Paneth cells together with mesenchymal cells provide niche factors for the adjacent epithelial stem cells.[17,18] Paneth cells have been implicated in the pathogenesis of CD of the small intestine, based on changes in cellular morphology and effector gene expression.[19–26] Furthermore, single nucleotide variations/polymorphisms (SNPs) in several genes associated in GWASs with susceptibility to CD, including *NOD2*/*CARD15* (microbial recognition), *AT16L1* (autophagy), and *XBP1* (ER stress) are proposed to impair Paneth cell function but a clear understanding of CD pathogenesis remains incomplete.[3,22,23,27]

Herein, we present evidence supporting that ITLN1 and ITLN2 each likely represent distinct subfamilies of intelectins in primates, based on notable differences in primary structure, including unique amino termini and changes in amino acid residues associated with glycan the glycan-binding activity of ITLN1. These findings in humans contrast with those in mice, where the mouse intelectin locus has expanded to include up to six Itln1-like paralogs depending upon strain.[28,29] Although numerically annotated in the literature like the human ITLNs, murid intelectins are all structural/functional orthologs of human ITLN1, and no ITLN2 ortholog has been reported in any strain. Our results further show that human ITLN2 is expressed in Paneth cells, where it localizes to secretory granules, and establish that ITLN2 is a highly abundant multimeric protein secreted into the lumen of the small intestine. In surgical specimens of ileal CD, *ITLN2* mRNA levels were significantly reduced compared to control specimens. We demonstrate that identified SNPs of the *ITLN2* gene, as well as those ascribed to neighboring *ITLN1* that are associated with CD risk, do not modify *ITLN2* expression.[3–9,30,31] Lastly, we report that metaplastic Paneth cells, which are commonly detected in ulcerative colitis (UC) and colonic CD, express ITLN2. These data establish a framework to advance the understanding of ITLN2 function in the intestine, including a possible role in the pathogenesis of CD.

2 | METHODS

2.1 | Human specimens and ethics statement

All protocols for human specimens were approved by the Institutional Review Board at The Cleveland Clinic Foundation (Cleveland, OH). Human studies abided by the Declaration of Helsinki principles. Tissue specimens were obtained from individuals undergoing surgery for Crohn's disease (CD), ulcerative colitis (UC), or non-CD/UC-related (control, CTRL) indications (i.e., colon cancer, bowel obstruction, and familial adenomatous polyposis). In all cases, informed consent was obtained and specimens were deidentified. Diagnoses were based on standard criteria using clinical, radiological, endoscopic, and histopathological findings as described.[19] Exclusion criteria included the diagnoses of backwash ileitis, indeterminate colitis, concurrent CMV, or *C. difficile* infection. Samples were immediately either snap-frozen in liquid nitrogen (for RNA, DNA, and protein analysis) or placed into tissue fixative for histology. For mRNA and protein expression, the mucosa was dissected away from the intestinal/colonic serosa. Small intestinal lumen fluid/aspirates were obtained from patients undergoing colonoscopy and deidentified as previously described.[32] For tissue expression analysis, RNA was obtained from commercial sources; Biochain (Newark, CA) and Clonetech/Takara Bio (San Jose, CA).

2.2 | Databases

Investigation of the population frequency of SNPs: rs6680969, rs12730072, rs6701920, and others reported in Figure 6 and Table S1 utilized Ensembl Genome Browser and data from the 1000 Genomes Project (Phase 3).[33,34]

Initial identification of variants was performed using NCBI-ClinVar (https://www.ncbi.nlm.nih.gov/clinvar/), NCBI-LitVar (https://www.ncbi.nlm.nih.gov/CBBresearch/Lu/Demo/LitVar/#!?query=), and the reference NCBI page for *ITLN2* (gene ID: 142683) in conjunction with NCBI-dbSNP (https://www.ncbi.nlm.nih.gov/snp/).[35–37] Linkage disequilibrium between identified SNPs was performed using NCBI-LDlink toolsets: LDpair (https://ldlink.nci.nih.gov/?tab=ldpair) and LDtrait (https://ldlink.nci.nih.gov/?tab=ldtrait).[38]

2.3 | RNA isolation and cDNA synthesis

The general procedures for RNA isolation and synthesis of cDNA were previously described by our group.[19,39] For the current study, RNA was freshly isolated for all specimens from stocks of frozen tissue maintained at −80°C.[19] As was described in detail,[9,19,39,40] total RNA was isolated using cesium chloride gradient ultracentrifugation, quantified using ultraviolet absorption spectrometry at 260 nm, and reverse transcribed to cDNA using the SuperScript™ III First-Strand Synthesis System (ThermoFischer, Waltham, MA; #18080051). The single-stranded cDNA product was purified using a Qiagen PCR purification kit (Qiagen, Valencia, CA; #28106), and diluted to 10 ng/μl based on the input concentration of the total RNA.

2.4 | Quantitative real-time PCR

For quantitative real-time PCR (qRT-PCR), cDNA templates corresponding to 10 ng of specimen RNA were used and reactions were monitored using a Roche Diagnostics Lightcycler 2.0 (Roche, Indianapolis, IN) and SYBR Green product detection, as previously described.[19,39,40] Absolute quantification of specific mRNA from tissue was determined by extrapolation of the detection threshold (crossing point) to the crossing point for gene-specific external plasmid cDNA standards analyzed within each PCR analysis. A negative control reaction that omitted template cDNA was included with each set of PCR reactions. Target-specific amplification was confirmed by DNA sequence analysis of the PCR products. Reproducibility assessments of the quantitative approach were previously reported.[39] Briefly, for assessment of intra-sample reproducibility, RNA from multiple specimens was used to synthesize, isolate, and purify cDNA templates in quadruplicate; the qRT-PCR analysis of these templates determined that ratios of a standard deviation relative to the mean of measured target mRNA levels was approximately 15%. The variability observed for individual samples assayed in separate reactions on different days was approximately 10%, and the variability observed for replicates of samples within a single reaction was also approximately 10%. Oligonucleotide primers were designed using MacVector Software (https://macvector.com/), and as previously reported[9,19,39]: *ITLN1* (f: 5′-CTTCGTCTCCATCTCTGCCC-3′, r: 5′-CTGGTAGATAACACCATTCTC-3′), *ITLN2* (f: 5′-GCCTCCTCCTTTTCTTCCCTGCCTAG-3′, r: 5′-GGTCTGGTAGACAACACCATTCTCG-3′), *DEFA5* (f: 5′-TGGGGAAGACAACCAGGACC-3′, r: 5′-TTCGGCAATAGCAGGTGGC-3′), *DEFA6* (f: 5′-GCTTATGAGGCTGATGCCCAG-3′, r: 5′-GGCAAGTGAAAGCCCTTGTTG-3′), *LYZ* (f: 5′-AAAACCCCAGGAGCAGTTAAT-3′, r: 5′-CAACCCTCTTTGCACAAGCT-3′) *REG3A* (f: 5′-CCCACTGCTATGCCTTGTTTTTGTC-3′, r: 5′-ACTGCTACTCCACTCCCAACCTTCTC-3′), and *SPLA2G2A* (f: 5′-CGCACTCAGTTATGGCTTCTACG-3′, r: 5′-AGGTGATTCTGCTCCCCGAG-3′). Conditions for qPCR: Initial denaturation at 95°C for 10 min, followed by 45 cycles with each cycle consisting of denaturation, 95°C for 15 s; annealing at 60°C for 5 s; and extension at 72°C for 10 s. Following the cycle runs, samples were denatured to establish the melting temperature(s) of the PCR product. The sample melt temperatures were compared to that of the internal standard to confirm template specificity.

2.5 | Genotype analysis

Genomic DNA was isolated, purified, and quantitated as described.[9,19] Evaluation of single nucleotide polymorphisms in *ATG16L1* (rs2241880) and *NOD2* (rs2066844, rs2066845, and rs2066847) were determined by PCR amplification of genomic DNA across adjacent regions, followed by Sanger sequencing using a protocol previously described.[9,19] Variants of *ITLN2* present in our cohort (rs12730072 and rs6680969) were identified with the same approach using the primers: f: 5′-AGAAATCAGCACCCAGTCC-3′ and r: 5′-GAGAGAGAGAGAACACGAAAG-3′. Exon variants were explored by Sanger sequencing of cDNA corresponding to the coding region of *ITLN2* amplified using gene-specific primers (f: 5′-TCCGAGTGTCCACAGGAAGGGA-3′ and r: 5′-CAAATAGCCGGGGTTGGAAGAT-3′). The sequenced PCR products were aligned to the NCBI-*ITLN2* reference (NM_080878), identifying a single variation, rs6680969 (C/T), in some specimens. For these analyses, the PCR reactions were initiated by denaturation of the DNA template at 95°C for 10 min followed by 45 cycles consisting of 95°C for 15 s, a −1°C per two-cycle "touchdown" annealing temperature for 5 s (i.e., 65–58°C), and 10 s at 72°C.

2.6 | Antibodies

Analysis of the deduced protein sequence of the entire open reading frame of ITLN2 using the SignalP5.0 algorithm indicated signal sequence proteolytic cleavage would occur between A26 and A27.[41] The adjacent 21 amino acids of ITLN2 (AAASSLEMLSREFETCAFSFS) comprised a completely unique sequence compared to the corresponding region of the human ITLN1 sequence (WSTDEANTYFKEWTCSSSP). Adjacent to this discriminating 21-amino acid sequence (A27 to S47) of ITLN2 is a domain beginning at amino acid S48 that has a very high sequence identity to ITLN1 as well as other intelectin orthologs. BLASTp search of the non-redundant protein database with the 21-amino acid peptide sequence (A27 to S47) yielded numerous primate ITLN2 orthologs with highly similar sequences (70%–100%), but no other mammalian proteins. This 21-amino acid peptide was used to immunize rabbits by a protocol described in detail.[9] Briefly, the synthetically prepared peptide was coupled to ovalbumin (separately using glutaraldehyde and maleimide) and independently to keyhole limpet hemocyanin (KLH, again separately using glutaraldehyde and maleimide). Rabbits were immunized by Antibodies Inc. (Davis, CA) with the ITLN2 peptide/OVA antigen on days 1, 14, 21, and then boosted by immunization with ITLN2 peptide/KLH antigen on days 35 and 49 to produce the N-terminal polyclonal antisera (termed ITLN2^{NTERM}). Preimmunization sera were collected and used as control antisera. All methods for these procedures were in accordance with relevant guidelines and regulations and approved by the U.S. Department of Health and Human Services Public Health Service Animal Welfare Assurance Committee (Assurance ID D16-00576).

A chicken IgY anti-ITLN^{CONS} preparation was generated using a 28 aa peptide (CTVGDRWSSQQGSKA DYPEGDGNWANYN) corresponding to a conserved region of human ITLN1 that has 27 of 28 identical residues in human ITLN2, as described.[9] Briefly, the peptide was coupled to KLH and then used as an antigen to immunize leghorn chickens (Aves Labs, Inc., Davis, CA).[9] A polyclonal antiserum (termed rabbit ITLN^{CONS}) was generated by immunization of rabbits with a 16 aa synthetic peptide (CTVGDRWSSQQGSKAD) from this same conserved protein region as described.[12,42]

2.7 | Immunoblot analysis

Ileal tissues were homogenized and analyzed as described.[9] Briefly, tissue was homogenized in RIPA buffer (150 mM NaCl, 1% Triton X-100, 0.5% sodium deoxycholate, 0.1% SDS, 50 mM Tris, pH 8.0) containing a cocktail of protease inhibitors (Protease Inhibitor Cocktail III) diluted 1:100 to yield final concentrations: 4-(2-aminoethyl) benzenesulfonyl fluoride (1 mM), aprotinin (800 nM), bestatin (50 μM), E-64 (15 μM), leupeptin (20 μM), pepstatin (10 μM) (Calbiochem/EMD Millipore, Burlington, MA; #539134). Protein concentration was determined by a bicinchoninic acid assay (ThermoFischer, Waltham, MA; #23225). Small intestinal fluid/aspirate was prepared as previously reported.[32] To further remove fecal contaminants, total protein was precipitated from aliquoted supernatants using the ReadyPrep™ 2-D Cleanup Kit (Bio-Rad Laboratories, Hercules, CA; #1632130) following the manufacturer's protocol. Washed protein pellets were resuspended in RIPA buffer containing protease inhibitors. Western blot preparation: samples were heated at 95°C for 30 min either with (reduced) or without (non-reduced) 2.5% v/v 2-mercaptoethanol; protein extracts (25–50 μg/lane) were loaded on SDS-polyacrylamide gels (10% and 4%–20% acrylamide) and electrophoresed for 40–50 min at 200 V, prior to wet transfer (Towbin Buffer: 25 mM Tris, 192 mM glycine, 20% v/v methanol, pH 8.3) to Amersham™ Protran™ 0.1 μM nitrocellulose membranes (Millipore Sigma, Burlington, MA; #GE10600000) at 350 mA for 60–80 min. MagicMark™ XP Western Protein Standards (ThermoFischer, Waltham, MA; #LC5602), containing recombinant proteins that contain IgG binding sites were used to estimate molecular sizes. Membranes were blocked in PBS-T containing 5% w/v skim milk for 30 min and incubated with primary antibodies at 4°C. Following overnight incubation, membranes were washed with PBS-T for 1 h, probed with donkey anti-rabbit IgG horseradish peroxidase (HRP) linked secondary antibody (Millipore Sigma, Burlington, MA; #NA934) for 3 h at room temperature, rinsed in PBS-T, and visualized using SuperSignal™ West Femto chemiluminescent substrate (ThermoFischer, Waltham, MA; #34094). Chemiluminescent signal was detected using a Biospectrum AC Imaging System (UVP, Upland, CA).

2.8 | Immunohistochemistry

Human ileal and colonic tissues were fixed in either aqueous paraformaldehyde (PFA; 4% w/v), Carnoy's fixative, or HistoChoice™ Tissue Fixative (Millipore Sigma, Burlington, MA; #H2904). The fixed tissues were paraffin-embedded, sectioned (4–5 μm), and mounted on X-tra™ positive-charged slides (Leica Biosystems, Buffalo Grove, IL). Sections were deparaffinized in xylene, washed in denatured ETOH (95%), and rehydrated in 70% ETOH and H_2O. For PFA-fixed tissues, rehydrated specimens underwent an additional antigen

retrieval step, by incubation overnight at 60°C in sealed glass Coplin jars containing Tris-ETDA buffer (10 mM Tris base, 1 mM EDTA, and 0.05% Tween 20; pH 9.0). Thereafter, slides (all fixation types) were equilibrated in PBS (2 × 10 min) and blocked with 5% donkey serum (in PBS) for 30 min prior to overnight incubation at 4°C with primary antibodies.[9,39] To identify goblet cells, a mucin-2 (MUC2) antibody was used. The reagent was generated against peptides of the C-terminal domain (adjacent to the autocatalytic sequence) of the mature MUC2 protein ($MUC2^{C3}$), which localizes to granules and secreted material.[43] Following incubation, slides were washed, and probed with Vectastain ABC kit goat anti-rabbit or anti-mouse secondary antibodies (Vector Laboratories, Burlingame, CA; #PK-6101 and #PK-6102), activated with 3,3-diaminobenzidine peroxidase (Vector Laboratories, Burlingame, CA; #SK-4100), and counterstained in 0.4% light green (Millipore Sigma, Burlington, MA; #L5382) in 0.2% glacial acetic acid for 5 min prior to dehydration and mounting.[39] For light microscopy, slides were visualized using an Olympus BX51 microscope (Center Valley, PA). Images were processed using Adobe Creative Suite software.

2.9 | Fluorescence immunohistochemistry

Specimen slides were prepared as described above. Tissues were incubated overnight at 4°C with primary antibodies. After washing in PBS, specimens were incubated with a mixture of secondary antibodies (goat anti-chicken IgY Alexa Flour Plus 647 [Thermo Fischer Scientific, Waltham, MA; #A32933], goat anti-rabbit IgG Alexa Flour 488 [Abcam, Cambridge MA; #ab150077] and/or goat anti-mouse IgG Alexa Fluor Plus 647 [Thermo Fischer Scientific, Waltham, MA; #A32728]) for 1–2 h at room temperature. The slides were then rinsed and stained with DAPI using the TrueVIEW Autofluorescence Quenching Kit (Vector Laboratories, Burlingame, CA; #SP-8400-15) according to the manufacturer's protocol. Images were captured using a Leica SP8 STED 3X confocal microscope (Leica Microsystems Inc., Buffalo Grove, IL). Acquired Z-stacks and figure images were generated using Imaris (Oxford Instruments, Zurich, CH) and Fiji ImageJ (version 1.0, https://imagej.net/Fiji) software programs.[44]

2.10 | Statistical analysis

Statistical analysis was performed using GraphPad Prism software (version 9.0.0, GraphPad Software, San Diego, CA). Specific details are outlined in figure and table legends.

3 | RESULTS

A sequence comparison of ITLN2 and ITLN1 revealed 77% amino acid identity but illustrated some striking differences. Most notable were distinguishing features of the N-terminus (Figure 1A). Both proteins are predicted to have signal sequences (18 aa for ITLN1 and 26 aa for ITLN2, according to the SigPv5 algorithm prediction). Following signal sequence cleavage, ITLN1 is predicted to have 313 aa, while ITLN2 has 325 aa. Adjacent to the predicted cleavage site is a stretch of amino acids that delineate ITLN1 from ITLN2 (17 aa for ITLN1 and 20 aa for ITLN2) with the remainder of the mature proteins showing greater conservation (Figure 1A). Of note, intelectins from several non-human primates show essentially identical patterns of similarity for their orthologs of ITLN1 and ITLN2 (Figure 1A). As intelectins are calcium-dependent lectins, we searched for differences between ITLN1 and ITLN2 and across the known calcium- and carbohydrate-binding amino acid residues.[2] An alignment of representative intelectin proteins showed that all 10 calcium-binding residues are perfectly conserved in the primary sequence of both ITLN1-like and ITLN2-like proteins (Figure 1B). The eight amino acids involved in carbohydrate-binding in human ITLN1 (residues 243, 244, 260, 262, 263, 274, 288, and 297; highlighted in yellow) are identical in mouse Itln1, consistent with biochemical studies showing comparable glycan-binding specificity for these two proteins (Figure 1B).[2,29] The ITLN1 orthologs in chimpanzee, gorilla, bonobo, and baboon have identical residues at these positions (black font); however, two positions differ in ITLN2 (E274Q and Y297S). In addition to these differences, there are four additional amino acid residue differences in this domain between the ITLN1 and ITLN2 sequences (arrowheads) (Figure 1B). These sequence differences in ITLN2 might directly (i.e., ligand interaction) or indirectly (i.e., configuration of binding pocket) modify glycan binding and suggest different carbohydrate-ligand specificity between ITLN1 and ITLN2.

Other than northern blot data detecting *ITLN2* mRNA in the small intestine reported two decades ago, mRNA quantification, protein expression, and cellular source(s) have not been characterized.[14] Therefore, we generated *ITLN1* and *ITLN2*-specific qRT-PCR assays to enable absolute quantification of mRNA transcript across tissues. Human *ITLN2* mRNA was present at high levels in the small intestine but found to be either non-detectable or minimally expressed (i.e., 100–1000-fold lower levels) in the colon and extra-intestinal tissues. In contrast, *ITLN1* was highly expressed in several tissue types, including the small intestine, colon, visceral adipose,

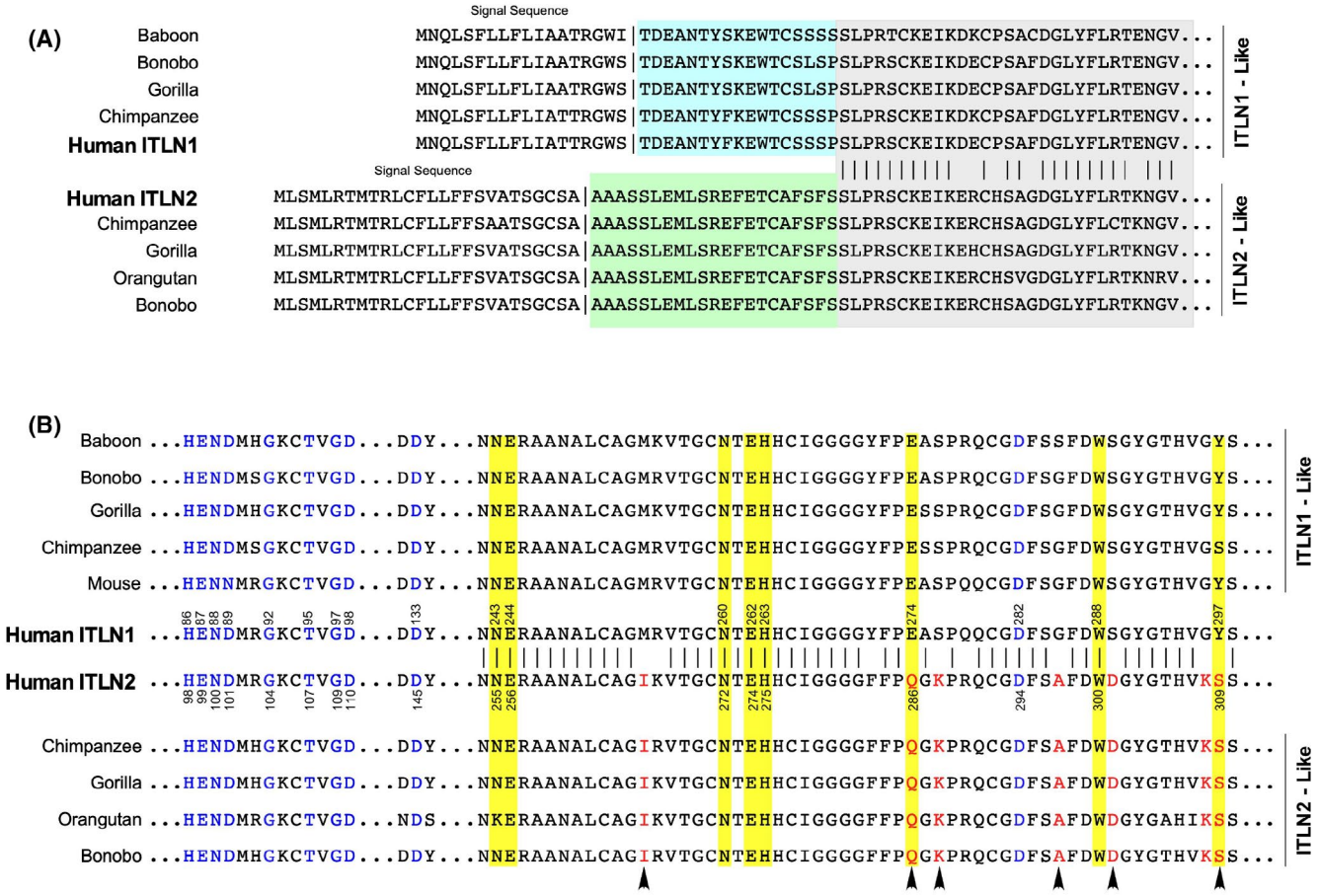

FIGURE 1 Comparison of the N-terminal amino acid sequence and the calcium- and glycan-binding residues of selected intelectins. The aligned partial amino acid sequences of intelectins from human, mouse, and selected primates are shown. (A) N-terminal amino acid sequences of human ITLN1 and ITLN2 aligned with intelectins of other primates. Signal sequences were predicted with the SigP v5.0 algorithm.[41] Amino acids at the N-terminus of primate ITLN1 proteins are perfectly conserved (blue box). Similarly, amino acids at the N-terminus of primate ITLN2 proteins are perfectly conserved (green box) but share little or no similarity with ITLN1 sequences. The adjacent sequence is similar for both ITLN1 and ITLN2 proteins (gray box). Identical residues are indicated with vertical lines. (B) Amino acids previously shown from ITLN1 to mediate calcium coordination are shown in blue and those mediating glycan binding are highlighted with yellow.[2] Each of the residues mediating calcium coordination (86–89, 92, 95, 97, 98, 133, and 282) in human ITLN1 is conserved in all sequences analyzed. The eight residues previously shown to bind carbohydrates (243, 244, 260, 262, 263, 274, 288, and 297) in human ITLN1 and mouse Itln1 are conserved in the other ITLN1 sequences analyzed (shown in black within the yellow background). The two residues that differ in ITLN2 compared to ITLN1 are shown in red within the yellow background. The six polymorphic residues in this region between the ITLN1 and ITLN2 sequences are designated with arrowheads. Amino acid residue numbering for human ITLN1 and ITLN2 are shown above or below their respective sequence. The deduced amino acid sequences were retrieved with the following accession numbers: *Homo sapiens* (human) ITLN1 (NP_060095) and ITLN2 (NP_543154); *Pan troglodytes* (chimpanzee) ITLN1 (XP_016786116) and ITLN2 (XP_513929); *Pan paniscus* (bonobo) ITLN1 (XP_003811911) and ITLN2 (XP_003811909); *Pongo abelii* (orangutan) ITLN1 (XP_002809985) and ITLN2 (XP_009240277); *Papio anubis* (baboon) ITLN1 (XP_003892986); and *Mus musculus* (mouse) Itln1 (NP_034714)

uterus, and lung (Figure 2A). The restricted expression of *ITLN2* in the small intestine mirrored that of Paneth cell effectors, including the highly abundant antimicrobial α-defensins, *DEFA5* (HD5), and *DEFA6* (HD6) (Figure 2B).[39,45–49]

We next investigated protein profiles in surgical specimens of the human ileum, a site of high expression for both *ITLN1* and *ITLN2*. Using an antibody targeting a conserved region in both paralogs (ITLN conserved, ITLN^{CONS}) two distinct bands of ~35 and ~40 kDa were observed under reducing conditions by SDS-PAGE and present in both ileal tissue and lumen fluid/aspirate (Figures 2C and S1A).[42,50] We employed paralog-specific antibodies generated against the unique N-terminal sequences described above of ITLN1 (ITLN1^{NTERM}) and ITLN2 (ITLN2^{NTERM}) to elucidate the electrophoresis profiles of each isoform.[9] Under reducing conditions, ITLN1^{NTERM} staining was present at ~40 kDa, whereas ITLN2^{NTERM} appeared at ~35 kDa (Figure 2D). Our results from human tissue are consistent with findings by

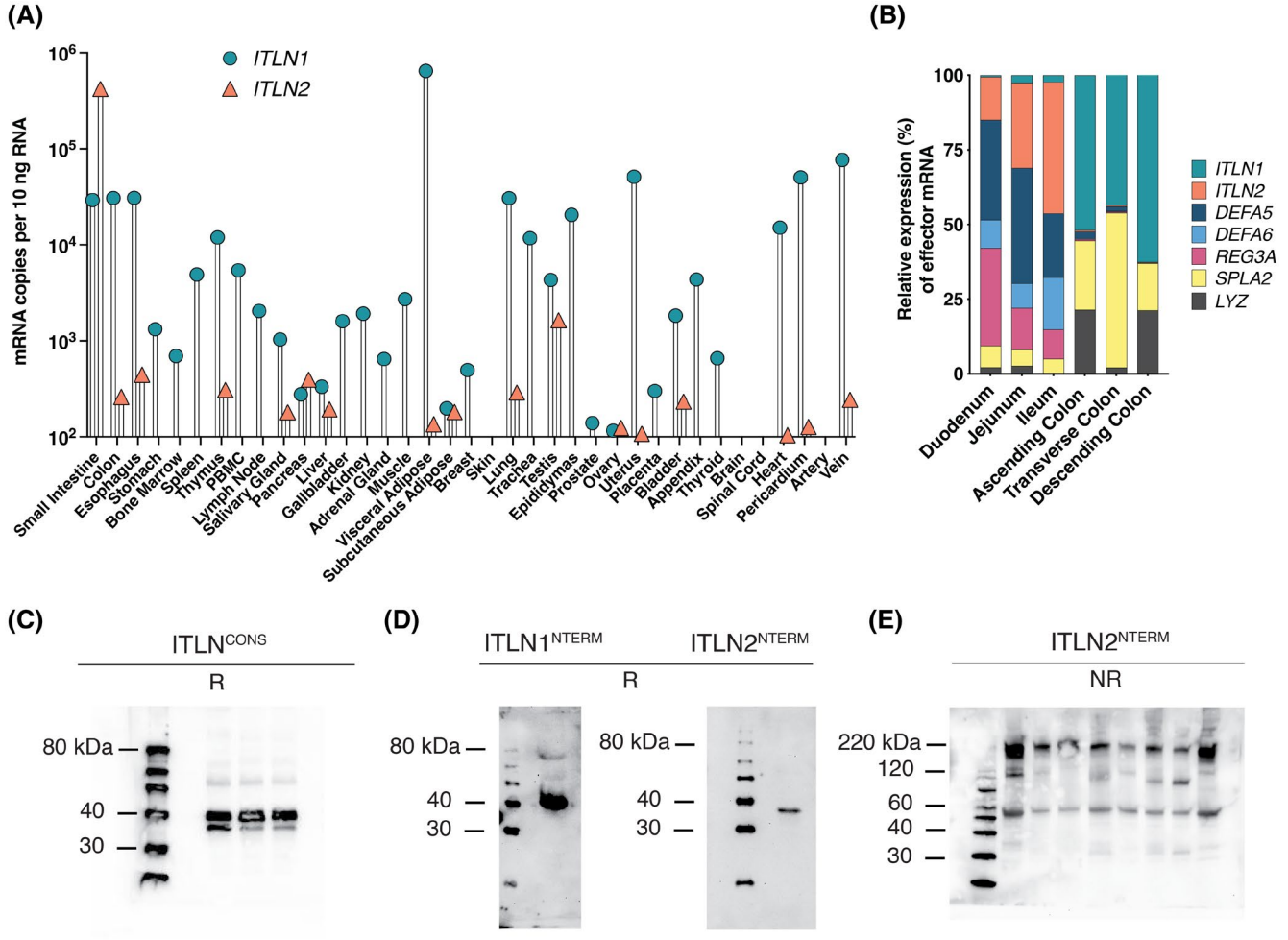

FIGURE 2 Human ITLN2 is highly expressed in the small intestine. (A) *ITLN1* and *ITLN2* mRNA expression in human tissues (see methods for details). (B) Relative expression of *ITLN2* and other epithelial cell effector proteins in the small intestine and colon. The proportion of mRNA transcript encoding each protein is plotted as the percentage of transcript total for these molecules at each location. (C) Immunoblot of human ileal tissue from three individuals under reducing conditions (R) using an antibody recognizing both ITLN1 and ITLN2 (i.e., ITLN^{CONS}). (D) Representative immunoblots under reducing conditions of ITLN1 and ITLN2 using paralog-specific antibodies (i.e., ITLN1^{NTERM} and ITLN2^{NTERM}). The representative blot depicts a sample run in duplicate on a single nitrocellulose membrane that was cut prior to antibody incubation to display mobility differences between paralogs. (E) Immunoblot of human ileal tissue ($n = 8$) under non-reducing conditions (NR) using a gradient (4%–20%) SDS-PAGE and ITLN2^{NTERM} antibody

Tsuji et al., where recombinant ITLN1 and ITLN2 migrated in denaturing gels at approximately ~40 and ~35 kDa, respectively.[51] Gradient SDS-PAGE (4%–20%), under non-reducing conditions, revealed a predominant band at approximately ~220 kDa, suggesting ITLN2 can form hexamers in addition to trimers (~105 kDa) in its quaternary structure (Figure 2E).

To delineate the cellular source of ITLN2, we utilized an immunohistochemical approach. Prominent crypt staining of ileum was observed with the ITLN^{cons} antibody (Figure S1B), suggestive of Paneth cells. Ileal Paneth cells were identified using a HD5 monoclonal antibody (HD5^{8C8}), which recognizes the pro-domain of the peptide (i.e., intracellular form) (Figure 3A).[52] ITLN2-specific (ITLN2^{NTERM}) staining mirrored that of HD5 and colocalized using confocal microscopy, where positive staining was observed within Paneth cell granules (Figure 3A,B). Paralog-specific staining further clarified that Paneth cell staining was due to ITLN2 (not ITLN1) and confirmed that ITLN1 is a goblet cell product in the small intestine (Figure S1C,D).[9]

Reduced expression of Paneth cell α-defensins has been reported in ileal CD and is proposed to contribute to dysbiosis associated with this disease.[19,23,24,53] We investigated mRNA transcript levels of *ITLN2* in a previously described cohort of surgical specimens from patients with colonic CD and UC.[9,19,25] In ileal CD specimens, *ITLN2* mRNA levels were approximately fivefold lower than in controls (Figure 4A). Expression levels of *ITLN2* mRNA correlated strongly with both *DEFA5* and *DEFA6* (Figure S2A).

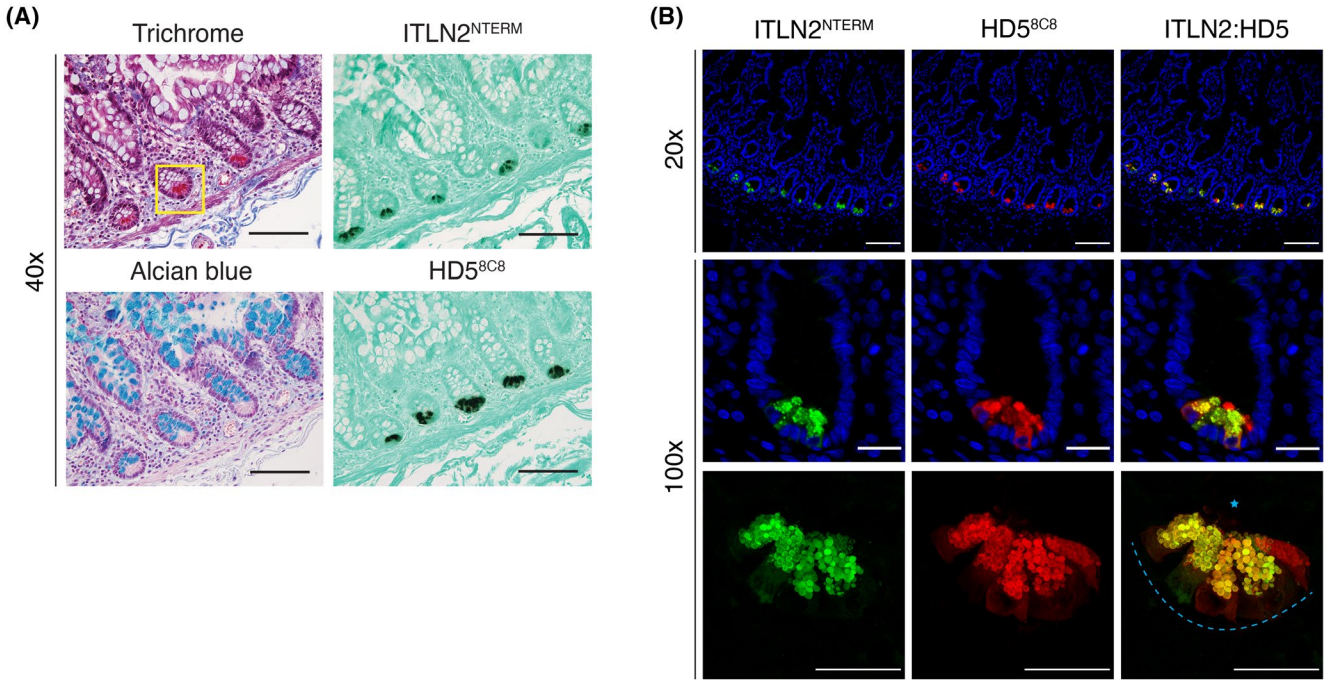

FIGURE 3 Human ITLN2 is a Paneth cell product. (A) Histology and immunohistochemistry of human ileum. Paneth cells are identified with Masson's trichrome (in the yellow box of upper left panel), and goblet cells by Alcian blue (lower left panel). ITLN2^{NTERM} and HD5^{8C8} staining of Paneth cells (right panels). (B) Immunofluorescent colocalization of ITLN2^{NTERM} and HD5^{8C8} staining in Paneth cells in the ileum. The dotted blue line outlines the basolateral surface of identified Paneth cells, and the star indicates luminal orientation. Scale bars: light microscopy 40× = 100 μm; fluorescence microscopy: 20× = 100 μm and 100× = 25 μm

ITLN2 mRNA expression was independent of genotype for GWAS-identified CD risk alleles *NOD2/CARD15* rs2066844 (R702W), rs2066845 (G908R), and rs2066847 (L1007fsX1008), as well as *ATG16L1* rs2241880 (T300A) (Figure 4B). Moreover, the expression levels were found to be independent of the histologic grade of inflammation (Figure S2B,C).[19,25]

The expression pattern of ITLN2 in the colon was quite different. *ITLN2* mRNA, undetectable in control samples, was present at high levels in colon specimens from patients with colonic CD or UC (Figure 5A). Paneth cell metaplasia rarely occurs distally to the ascending colon in healthy tissue; however, in colonic CD and UC, it occurs at frequencies upwards of 40% in the distal large bowel.[20,54] Consistent with Paneth cell metaplasia, *DEFA5* (HD5) mRNA, also undetectable in control specimens, was present at manifold higher levels in CD and UC colon samples (Figure 5A). Moreover, immunoreactivity for both HD5^{8C8} and ITLN2^{NTERM} was present in samples with high *DEFA5* and *ITLN2* mRNA expression (Figure 5B). These metaplastic Paneth cells were distributed across UC and CD tissue specimens (Figure S3A,B). Together, our findings support the concept that ITLN2, a Paneth cell product in the small intestine, is also a product of metaplastic Paneth cells in the colon. This clarification argues against the colonic source for ITLN2 as being an inducible gene product of goblet cells or another epithelial cell lineage.

To investigate a potential role of genetic variants of *ITLN2* in the context of CD, we sequenced the complete coding region of *ITLN2* in specimens of our cohort (n = 113) and mined databases for disease-associated SNPs ascribed to *ITLN2* (Table S1).[33,34,55] Our sample cohort revealed a single, common missense variant (C/T, rs6680969) resulting in a change from arginine to histidine at amino acid position 103 (R103H).[56] Assessment of the sequence at this position in ITLN1- and ITLN2-like orthologs in mammals suggests this residue is interchangeable, but in human ITLN1 the corresponding residue (R91) is not polymorphic (Figure 6A).[9,33,34] The allele frequency of rs6680969 (C/T) in our surgical cohort did not differ between control and CD groups (DNS) and mirrored that of European superpopulations (SP), where T (H103) is the major allele (Figure 6B and Table S1).[33,34]

There are two published disease-associated SNPs of *ITLN2*, both located in untranslated regions of the gene: rs12730072 (C/T) ~220 bp 5′ and rs6701920 (G/A) located ~102 bp 3′ (Figure 6B); the former associated with celiac disease and the latter with non-insulin-dependent diabetes mellitus (NIDDM).[30,31] Both rs12730072 and rs6701920 are rare allelic variants in global SP; 8% and 3%, respectively (Table S1). SNP rs12730072 occurs at the highest frequency in European SP (19%), whereas rs6701920 is largely restricted to African SP (12%) and was not present in our clinical specimen cohort (Figure 6B and

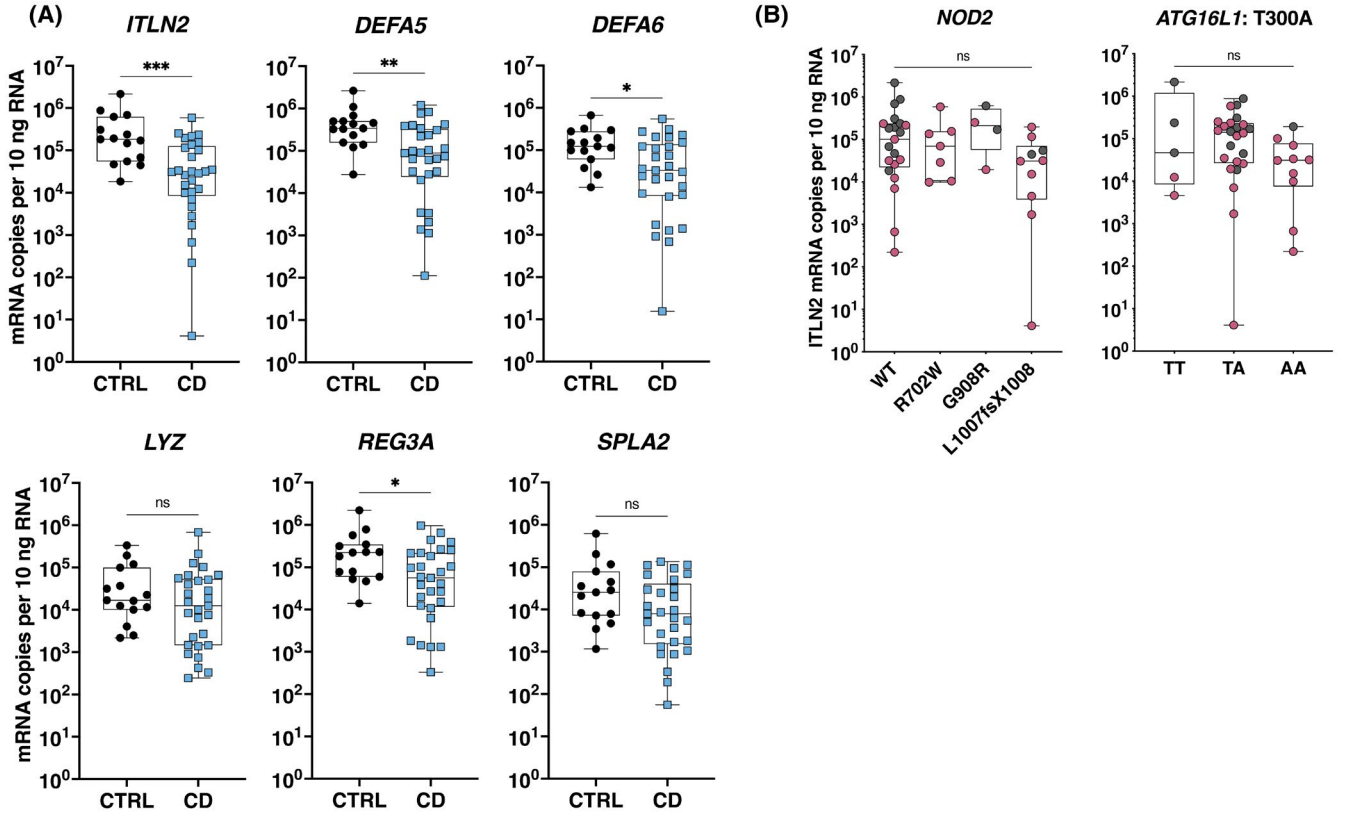

FIGURE 4 Human *ITLN2* mRNA expression is reduced in ileal CD but independent of inflammation and *NOD2* and *ATG16L1* genotype. (A) Gene expression of human *ITLN2* and other Paneth cell effectors in ileum from control ($n = 15$) and CD ($n = 29$) specimens. (B) *ITLN2* mRNA expression in ileum specimens by genotype for *NOD2*/*CARD15*: rs2066844 (R702W), rs2066845 (G908R), and rs2066847 (L1007fsX1008) (left panel) and *ATG16L1*: rs2241880 (T300A) (right panel); control = gray, CD = red. Box plots show the median and first and third quartiles, whiskers present the range. Statistical comparisons were performed by (A) Mann–Whitney *U* test or (B) Kruskal–Wallis test with Dunn's multiple comparisons post hoc: *$p < .05$, **$p < .01$, ***$p < .001$, ****$p < .0001$, ns = non-significant. CD, Crohn's disease; CTRL, control

Table S1).[33,34] Neither rs6680969 (R103H) nor rs12730072 influenced *ITLN2* mRNA expression in the ileum and thus did not yield further insight into the reduced expression levels observed in CD specimens (Figure 6C).

We previously reported that the multiple variants identified by GWAS at the *ITLN1* locus for CD are in linkage disequilibrium (LD) and form a "risk haplotype" in European SP, where disease-associated variants are major alleles.[3–9] Although not previously considered, we asked whether SNPs marking the CD-associated risk haplotype of *ITLN1* could be associated with the rs6680969 (R103H) variant of *ITLN2*, given that the global variant SP allele frequencies are similar (~50%) (Figure 6B and Table S1).[3,9,33,34] Genotype analysis of small intestine specimens within our study cohort revealed discordance of at least one allele in 29.8% (14/47) of individuals. Moreover, *ITLN2* mRNA expression levels in ileum were uninfluenced by the *ITLN1* genotype, stratifying for the *ITLN1* variant rs2274910 (C/T) as a marker for the risk haplotype (Figure 6C).[3,9] Together, these results indicate that variants of *ITLN1* associated with CD risk are likely independent of changes in ITLN2 biology, including reduced *ITLN2* mRNA expression in CD. Likewise, the missense variation in ITLN2 (R103H) is unlikely to explain the risk associated with CD at the *ITLN1* locus.

4 | DISCUSSION

Intelectins are calcium-dependent carbohydrate-binding proteins abundantly expressed at mucosal sites, including the small intestine and colon of mammals.[9,12,15,29,57–59] Humans encode two intelectins, ITLN1 and ITLN2, and each has respective orthologs in non-human primates. In the present study, we identify three discerning features of these proteins that together suggest ITLN1 and ITLN2 represent distinct subfamilies: (1) unique N-termini, (2) alternative residues at positions ascribed to carbohydrate-binding sites at the C-termini, and (3) cell type specificity within the intestine. In mice, the intelectin locus exhibits copy number variation, where up to six intelectin paralogs have arisen

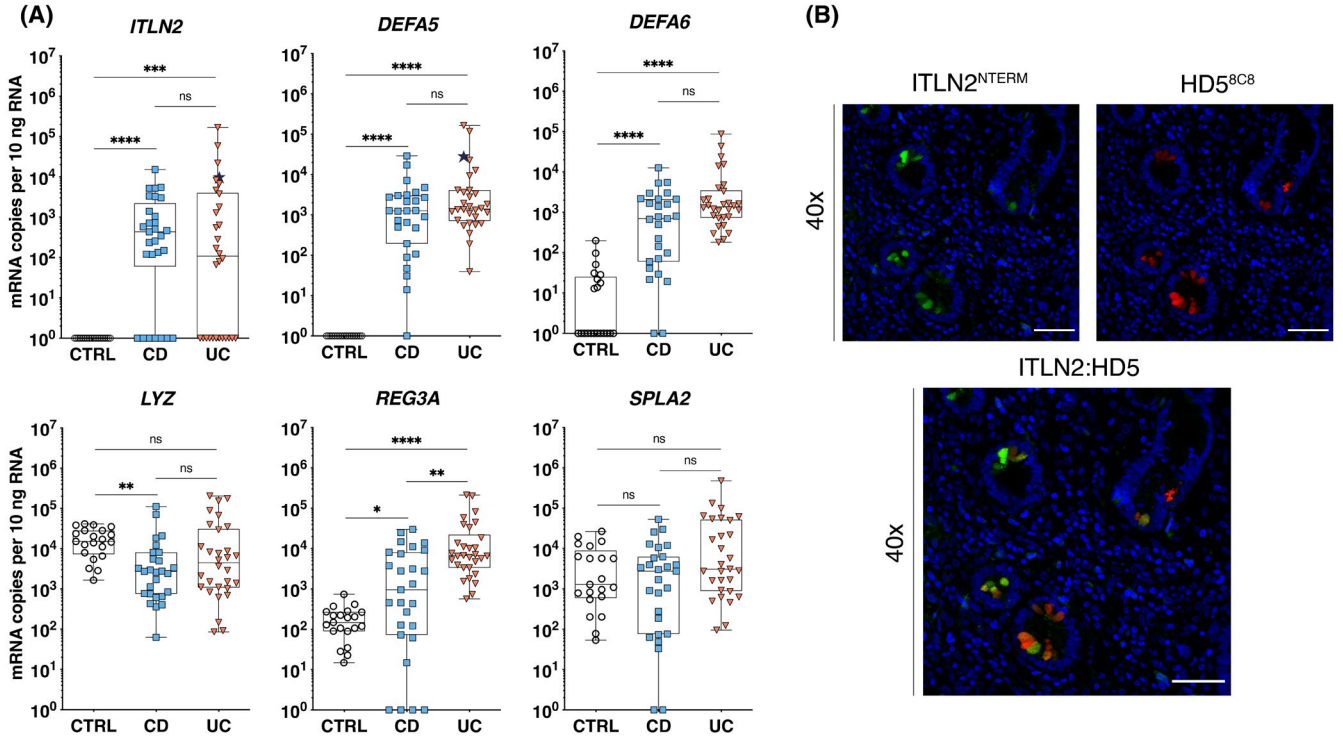

FIGURE 5 Colonic *ITLN2* expression in colonic CD and UC is reflective of Paneth cell metaplasia. (A) Transcript levels of *ITLN2* and other epithelial cell effectors in colon specimens (CTRL: $n = 21$, CD: $n = 27–29$, UC: $n = 29–30$). (B) Representative immunofluorescent colocalization of ITLN2^{NTERM} (green) and HD5^{8C8} (red) staining in colon of IBD specimens demonstrating presence of metaplastic Paneth cells. Star (★) symbol in *ITLN2* and *DEFA5* UC dataset indicates expression level for histological specimen in (B). Box plots show the median and first and third quartiles, whiskers present the range. Statistical comparisons were performed by Kruskal–Wallis test with Dunn's multiple comparisons post hoc: *$p < .05$, **$p < .01$, ***$p < .001$, ****$p < .0001$, ns = non-significant. CD, Crohn's disease; CTRL, control; UC, ulcerative colitis. Scale bars: 40× = 50 μm

from a common Itln1-like ancestor.[28,29] While orthologs of human ITLN2 are present in non-human primates as well as ungulates, they are absent in Murid rodents (Figure 6A).[29]

Little has been reported on human ITLN2 outside the initial identification of its mRNA by northern blot in the small intestine.[14] Herein, we report that ITLN2 is abundant and selectively expressed in the small intestine. Within the small intestine, ITLN2 expression is restricted to Paneth cells and localized to their secretory granules. *ITLN2* mRNA levels mirror the highly abundant human α-defensins, *DEFA5* (HD5) and *DEFA6* (HD6), also expressed in secretory granules of Paneth cells. Furthermore, in UC and colonic CD, ITLN2 is expressed in the colon, where its mRNA levels and cellular localization closely paralleled that of HD5, which has been previously shown to be a reliable and discerning marker for metaplastic Paneth cells.[52,60] Together, our data identify ITLN2 as a specific marker for both Paneth cells of the small intestine, as well as metaplastic Paneth cells in the descending colon, sigmoid, and rectum.

Human ITLN1 is not a Paneth cell product, but rather a goblet cell product in both the small and large intestine.[9,57] Curiously, Itln1, the murine ortholog of human ITLN1, is expressed by small intestinal Paneth cells.[15] To avoid confusion in the literature, it will be important to keep these distinctions clear—ITLN2 is expressed in Paneth cells but has no mouse ortholog; ITLN1 is expressed in goblet cells, whereas its mouse ortholog Itln1 is expressed in Paneth cells. Moreover, mouse Itln1 is largely restricted to the small intestine, while our data support that human ITLN1 is expressed at high levels in various extra-intestinal tissues, including visceral adipose, lung, and reproductive tract.[11,13,51,61,62] Lastly, and again in contrast to ITLN2, ITLN1-like family members appear to be inducible during Th2-type immune responses (e.g., parasitic infections and asthma).[13,59,63]

Human ITLN1 forms disulfide-linked homotrimers, which are postulated to enhance overall affinity and avidity to their target moiety, a vicinal 1,2-diol present on various microbial glycans.[2,10,12,64,65] Based on deduced amino acid sequence, mature ITLN1 has a predicted molecular weight slightly smaller than monomeric ITLN2 (32 881 vs. 33 342 Da); however, the N-linked glycosylation motif ascribed to ITLN1 (N163) by Tsuji, et al. is absent in the corresponding position of ITLN2.[51,64] Thus, N-linked

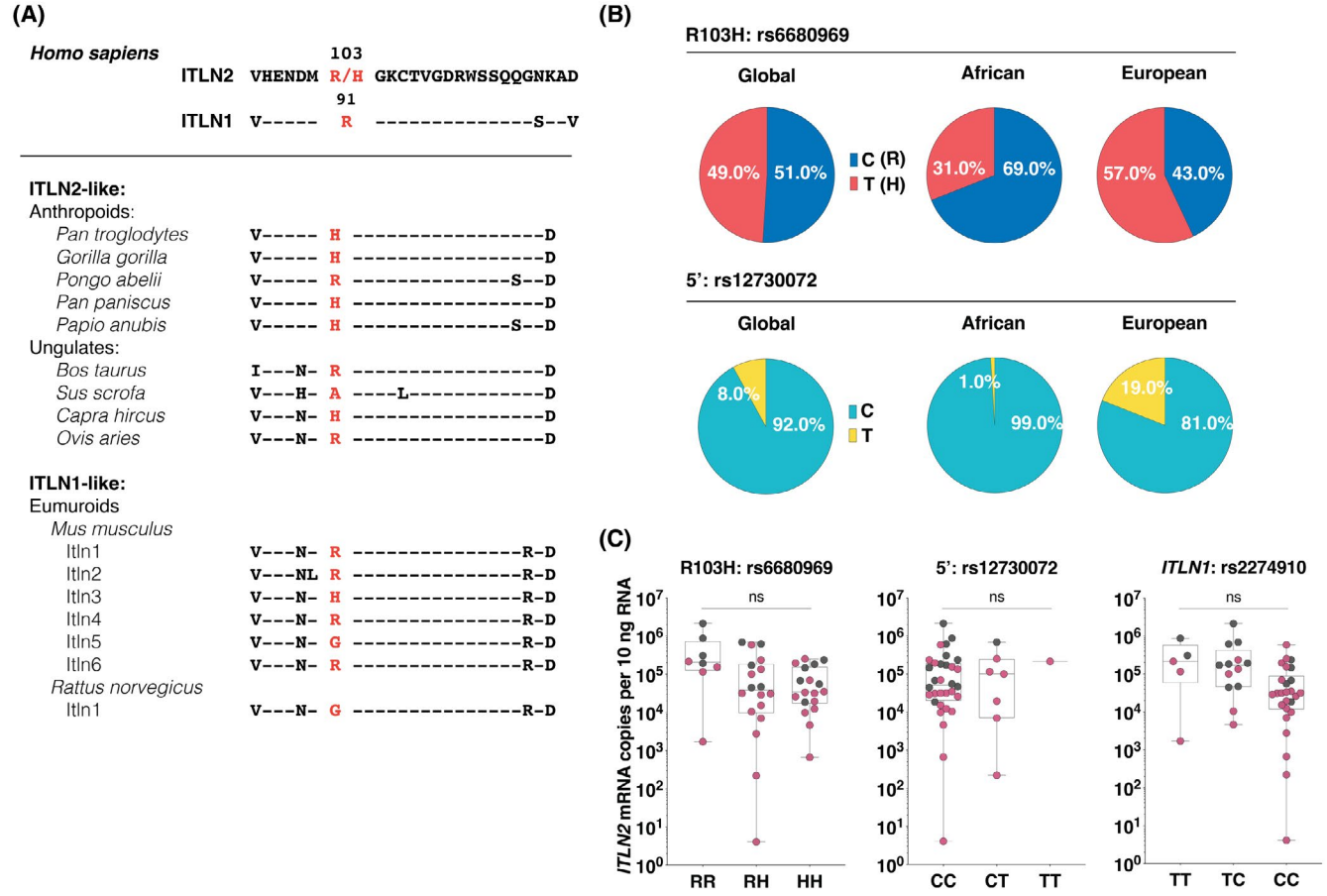

FIGURE 6 Overview of SNP variants of *ITLN2*. (A) Phylogenetic alignment of neighboring amino acids to missense variant R103H (rs6680969) of human ITLN2 ("—" identical residue present). (B) Allele frequencies of rs6680969 (C/T: R103H) and rs12730072 (C/T) in superpopulations as outlined by the 1000 Genomes Project (Phase 3).[33,34] (C) mRNA expression *ITLN2* in ileum by genotype: rs6680969 (R103H) and rs12730072; control = gray, CD = red. Box plots show the median and first and third quartiles, whiskers present the range. Statistical comparisons were performed by Kruskal–Wallis test with Dunn's multiple comparisons post hoc: ns = non-significant

glycosylation likely explains the slower electrophoretic mobility of ITLN1 than ITLN2 we detected in the present study. Intermolecular disulfides formed via C31 and C48, mediate homotrimer formation of human ITLN1.[2] These residues, as well as eight other cysteines forming four intramolecular disulfide bonds of ITLN1, have corresponding residues in ITLN2, suggesting similar folding and homotrimer formation of ITLN2. Furthermore, ITLN2 contains an additional cysteine near the C-terminus (C311) with an unknown function. We previously identified a hexamer species of human ITLN1; however, this confirmation is predicted to be independent of disulfide bonds due to the even pairing of available cysteines mediating intermolecular trimer formation.[2,9,66] Our electrophoresis data of human samples under non-reducing conditions suggests that ITLN2 also forms higher molecular weight oligomers, including a hexamer species. Previously, only a monomer species of ITLN2 that was recombinantly expressed had been reported.[51]

In the present study, we showed that ITLN2, an abundant Paneth cell product, exhibits lower mRNA expression in ileal CD, independent of the degree of tissue inflammation. Numerous studies have implicated changes in Paneth cell biology as a fundamental feature of small intestinal CD.[19–26,53] The attenuated expression of Paneth cell α-defensins, HD5 and HD6, previously reported was proposed to contribute to the dysbiosis associated with this disease.[19,23,53] This inflammation-independent reduction in α-defensin expression was particularly prominent in specimens with the 1005fs frameshift mutation in *NOD2* (rs2066847).[19,20,23] In the previous study, we showed the reduced expression of α-defensin in ileal CD specimens was selective, as eight other Paneth cell products were unaltered, including *SPINK1*, *LYZ*, *SERPINA1*, and *PRSS2*—the processing enzyme for proHD5 and proHD6.[19,67] Furthermore, α-defensin expression levels were unaltered in ileal specimens of inflamed pouchitis.[19] Like the α-defensins, the reduced expression of *ITLN2* mRNA in ileal CD specimens reported here was independent of inflammation; however, it was also independent of the three most common IBD-associated *NOD2*

variants, including 1005fs (rs2066847). Moreover, *ITLN2* expression levels were independent of IBD-associated SNPs in *ATG16L1* (rs2241880) and *ITLN1* (rs2274910).[3] Lastly, the expression levels of *ITLN2* in control and disease specimens were independent of identified SNPs in the *ITLN2* gene (rs6680969 and rs12730072). The possible functional consequences of reduced *ITLN2* expression in ileal CD require further study, but parallels of its expression patterns with those of Paneth cell α-defensins in CD are striking.

In conclusion, human ITLN2, an ortholog in a family of lectins with ancient evolutionary roots, has been largely neglected in the literature to date. The results reported here demonstrate the abundant and selective expression of ITLN2 in Paneth cells of the small intestine. ITLN2 colocalizes with the α-defensins in secretory granules of Paneth cells, and like HD5 and HD6, reduced expression of ITLN2 is observed in ileal CD. In contrast, ITLN1 is more broadly expressed, and in the small intestine and colon is expressed in goblet cells, where its expression is unaltered in CD.[9] Together, our findings suggest ITLN2, like ITLN1, has associations with CD. The precise biological role(s) of these effectors remain to be fully elucidated.

ACKNOWLEDGMENTS

We thank Dr. Carol A. De La Motte of the Cleveland Clinic for providing samples for histological analysis and Dr. Ingrid Brust-Mascher at the Health Sciences District Advanced Imaging Facility (UC Davis) for assistance with confocal microscopy. Funding sources: National Institutes of Health U01AI125926 (Mucosal Immunology Study Team) and R37AI32738.

DISCLOSURES

The authors stated explicitly that they have no conflicts of interest in connection with this article.

AUTHOR CONTRIBUTIONS

Conceptualization/design of research: Eric B. Nonnecke, Bo Lönnerdal, and Charles L. Bevins Performed research: Eric B. Nonnecke and Patricia A. Castillo Contributed new reagents, resources, and analytical tools: Malin E. V. Johansson, Edward J. Hollox, and Bo Shen Analyzed data: All authors. Wrote the paper: Eric B. Nonnecke and Charles L. Bevins Review and edited the paper: All authors.

ETHICS STATEMENT

The content is solely the responsibility of the authors and does not necessarily represent the official views of the National Institutes of Health.

DATA AVAILABILITY STATEMENT

The data that support the findings of this study are available in the methods and/or supplementary material of this article.

ORCID

Eric B. Nonnecke https://orcid.org/0000-0001-5345-2009
Charles L. Bevins https://orcid.org/0000-0003-2725-2622

REFERENCES

1. Chen L, Li J, Yang G. A comparative review of intelectins. *Scand J Immunol*. 2020;92:e12882.
2. Wesener DA, Wangkanont K, McBride R, et al. Recognition of microbial glycans by human intelectin-1. *Nat Struct Mol Biol*. 2015;22:603-610.
3. Barrett JC, Hansoul S, Nicolae DL, et al. Genome-wide association defines more than 30 distinct susceptibility loci for Crohn's disease. *Nat Genet*. 2008;40:955-962.
4. Franke A, McGovern DP, Barrett JC, et al. Genome-wide meta-analysis increases to 71 the number of confirmed Crohn's disease susceptibility loci. *Nat Genet*. 2010;42:1118-1125.
5. de Lange KM, Moutsianas L, Lee JC, et al. Genome-wide association study implicates immune activation of multiple integrin genes in inflammatory bowel disease. *Nat Genet*. 2017;49:256-261.
6. Jostins L, Ripke S, Weersma RK, et al. Host-microbe interactions have shaped the genetic architecture of inflammatory bowel disease. *Nature*. 2012;491:119-124.
7. Ellinghaus D, Jostins L, Spain SL, et al. Analysis of five chronic inflammatory diseases identifies 27 new associations and highlights disease-specific patterns at shared loci. *Nat Genet*. 2016;48:510-518.
8. Liu JZ, van Sommeren S, Huang H, et al. Association analyses identify 38 susceptibility loci for inflammatory bowel disease and highlight shared genetic risk across populations. *Nat Genet*. 2015;47:979-986.
9. Nonnecke EB, Castillo PA, Dugan AE, et al. Human intelectin-1 (ITLN1) genetic variation and intestinal expression. *Sci Rep*. 2021;11:12889.
10. Tsuji S, Uehori J, Matsumoto M, et al. Human intelectin is a novel soluble lectin that recognizes galactofuranose in carbohydrate chains of bacterial cell wall. *J Biol Chem*. 2001;276:23456-23463.
11. Schäffler A, Neumeier M, Herfarth H, Fürst A, Schölmerich J, Büchler C. Genomic structure of human omentin, a new adipocytokine expressed in omental adipose tissue. *Biochim Biophys Acta*. 2005;1732:96-102.
12. Suzuki YA, Shin K, Lönnerdal B. Molecular cloning and functional expression of a human intestinal lactoferrin receptor. *Biochemistry*. 2001;40:15771-15779.
13. Kerr SC, Carrington SD, Oscarson S, et al. Intelectin-1 is a prominent protein constituent of pathologic mucus associated with eosinophilic airway inflammation in asthma. *Am J Respir Crit Care Med*. 2014;189:1005-1007.
14. Lee JK, Schnee J, Pang M, et al. Human homologs of the Xenopus oocyte cortical granule lectin XL35. *Glycobiology*. 2001;11:65-73.

15. Komiya T, Tanigawa Y, Hirohashi S. Cloning of the novel gene intelectin, which is expressed in intestinal Paneth cells in mice. *Biochem Biophys Res Commun*. 1998;251:759-762.
16. Bevins CL, Salzman NH. Paneth cells, antimicrobial peptides and maintenance of intestinal homeostasis. *Nat Rev Microbiol*. 2011;9:356-368.
17. Clevers HC, Bevins CL. Paneth cells: maestros of the small intestinal crypts. *Annu Rev Physiol*. 2013;75:289-311.
18. van Es JH, Jay P, Gregorieff A, et al. Wnt signalling induces maturation of Paneth cells in intestinal crypts. *Nat Cell Biol*. 2005;7:381-386.
19. Wehkamp J, Salzman NH, Porter E, et al. Reduced Paneth cell alpha-defensins in ileal Crohn's disease. *Proc Natl Acad Sci USA*. 2005;102:18129-18134.
20. Wehkamp J, Harder J, Weichenthal M, et al. NOD2 (CARD15) mutations in Crohn's disease are associated with diminished mucosal α-defensin expression. *Gut*. 2004;53(11):1658-1664. doi:10.1136/gut.2003.032805
21. Stappenbeck TS, McGovern DPB. Paneth cell alterations in the development and phenotype of Crohn's disease. *Gastroenterology*. 2017;152:322-326.
22. Adolph TE, Tomczak MF, Niederreiter L, et al. Paneth cells as a site of origin for intestinal inflammation. *Nature*. 2013;503:272-276.
23. Wehkamp J, Stange EF. An update review on the Paneth cell as key to ileal Crohn's disease. *Front Immunol*. 2020;11:646.
24. Liu TC, Gurram B, Baldridge MT, et al. Paneth cell defects in Crohn's disease patients promote dysbiosis. *JCI Insight*. 2016;1:e86907.
25. Wehkamp J, Wang G, Kübler I, et al. The Paneth cell alpha-defensin deficiency of ileal Crohn's disease is linked to Wnt/Tcf-4. *J Immunol*. 2007;179:3109-3118.
26. Khaloian S, Rath E, Hammoudi N, et al. Mitochondrial impairment drives intestinal stem cell transition into dysfunctional Paneth cells predicting Crohn's disease recurrence. *Gut*. 2020;69:1939-1951.
27. Cadwell K, Liu JY, Brown SL, et al. A key role for autophagy and the autophagy gene Atg16l1 in mouse and human intestinal Paneth cells. *Nature*. 2008;456:259-263.
28. Lu ZH, di Domenico A, Wright SH, Knight PA, Whitelaw CB, Pemberton AD. Strain-specific copy number variation in the intelectin locus on the 129 mouse chromosome 1. *BMC Genom*. 2011;12:110.
29. Almalki F, Nonnecke EB, Castillo PA, et al. Extensive variation in the intelectin gene family in laboratory and wild mouse strains. *Sci Rep*. 2021;11:15548.
30. Senapati S, Sood A, Midha V, et al. Shared and unique common genetic determinants between pediatric and adult celiac disease. *BMC Med Genomics*. 2016;9:44.
31. Jablonski KA, McAteer JB, de Bakker PI, et al. Common variants in 40 genes assessed for diabetes incidence and response to metformin and lifestyle intervention in the diabetes prevention program. *Diabetes*. 2010;59:2672-2681.
32. Chairatana P, Chu H, Castillo PA, Shen B, Bevins CL, Nolan EM. Proteolysis triggers self-assembly and unmasks innate immune function of a human α-defensin peptide. *Chem Sci*. 2016;7:1738-1752.
33. Yates AD, Achuthan P, Akanni W, et al. Ensembl 2020. *Nucleic Acids Res*. 2020;48:D682-D688.
34. Auton A, Abecasis GR, Altshuler DM, et al. A global reference for human genetic variation. *Nature*. 2015;526(7571):68-74. doi:10.1038/nature15393
35. Allot A, Peng Y, Wei CH, Lee K, Phan L, Lu Z. LitVar: a semantic search engine for linking genomic variant data in PubMed and PMC. *Nucleic Acids Res*. 2018;46:W530-W536.
36. Landrum MJ, Lee JM, Benson M, et al. ClinVar: improving access to variant interpretations and supporting evidence. *Nucleic Acids Res*. 2018;46:D1062-D1067.
37. Sherry ST, Ward M, Sirotkin K. dbSNP—database for single nucleotide polymorphisms and other classes of minor genetic variation. *Genome Res*. 1999;9:677-679.
38. Machiela MJ, Chanock SJ. LDlink: a web-based application for exploring population-specific haplotype structure and linking correlated alleles of possible functional variants. *Bioinformatics*. 2015;31:3555-3557.
39. Wehkamp J, Chu H, Shen B, et al. Paneth cell antimicrobial peptides: topographical distribution and quantification in human gastrointestinal tissues. *FEBS Lett*. 2006;580:5344-5350.
40. Castillo PA, Nonnecke EB, Ossorio DT, et al. An experimental approach to rigorously assess paneth cell α-defensin (Defa) mRNA expression in C57BL/6 mice. *Sci Rep*. 2019;9:13115.
41. Almagro Armenteros JJ, Tsirigos KD, Sønderby CK, et al. SignalP 5.0 improves signal peptide predictions using deep neural networks. *Nat Biotechnol*. 2019;37:420-423.
42. Lopez V, Kelleher SL, Lonnerdal B. Lactoferrin receptor mediates apo- but not holo-lactoferrin internalization via clathrin-mediated endocytosis in trophoblasts. *Biochem J*. 2008;411:271-278.
43. Johansson ME, Phillipson M, Petersson J, Velcich A, Holm L, Hansson GC. The inner of the two Muc2 mucin-dependent mucus layers in colon is devoid of bacteria. *Proc Natl Acad Sci USA*. 2008;105:15064-15069.
44. Schindelin J, Arganda-Carreras I, Frise E, et al. Fiji: an open-source platform for biological-image analysis. *Nat Methods*. 2012;9:676-682.
45. Salzman NH, Ghosh D, Huttner KM, Paterson Y, Bevins CL. Protection against enteric salmonellosis in transgenic mice expressing a human intestinal defensin. *Nature*. 2003;422:522-526.
46. Chu H, Pazgier M, Jung G, et al. Human α-defensin 6 promotes mucosal innate immunity through self-assembled peptide nanonets. *Science*. 2012;337:477-481.
47. Jones DE, Bevins CL. Paneth cells of the human small intestine express an antimicrobial peptide gene. *J Biol Chem*. 1992;267:23216-23225.
48. Porter EM, Liu L, Oren A, Anton PA, Ganz T. Localization of human intestinal defensin 5 in Paneth cell granules. *Infect Immun*. 1997;65:2389-2395.
49. Jones DE, Bevins CL. Defensin-6 mRNA in human Paneth cells: implications for antimicrobial peptides in host defense of the human bowel. *FEBS Lett*. 1993;315:187-192.
50. Suzuki YA, Wong H, Ashida KY, Schryvers AB, Lönnerdal B. The N1 domain of human lactoferrin is required for internalization by caco-2 cells and targeting to the nucleus. *Biochemistry*. 2008;47:10915-10920.
51. Tsuji S, Tsuura Y, Morohoshi T, et al. Secretion of intelectin-1 from malignant pleural mesothelioma into pleural effusion. *Br J Cancer*. 2010;103:517-523.

52. Shen B, Porter EM, Reynoso E, et al. Human defensin 5 expression in intestinal metaplasia of the upper gastrointestinal tract. *J Clin Pathol*. 2005;58:687-694.
53. Salzman NH, Hung K, Haribhai D, et al. Enteric defensins are essential regulators of intestinal microbial ecology. *Nat Immunol*. 2010;11:76-83.
54. Tanaka M, Saito H, Kusumi T, et al. Spatial distribution and histogenesis of colorectal Paneth cell metaplasia in idiopathic inflammatory bowel disease. *J Gastroenterol Hepatol*. 2001;16:1353-1359.
55. Buniello A, MacArthur JAL, Cerezo M, et al. The NHGRI-EBI GWAS Catalog of published genome-wide association studies, targeted arrays and summary statistics 2019. *Nucleic Acids Res*. 2019;47:D1005-D1012.
56. Gerhard DS, Wagner L, Feingold EA, et al. The status, quality, and expansion of the NIH full-length cDNA project: the Mammalian Gene Collection (MGC). *Genome Res*. 2004;14:2121-2127.
57. Wang Y, Song W, Wang J, et al. Single-cell transcriptome analysis reveals differential nutrient absorption functions in human intestine. *J Exp Med*. 2020;217.
58. Wrackmeyer U, Hansen GH, Seya T, Danielsen EM. Intelectin: a novel lipid raft-associated protein in the enterocyte brush border. *Biochemistry*. 2006;45:9188-9197.
59. Pemberton AD, Knight PA, Gamble J, et al. Innate BALB/c enteric epithelial responses to Trichinella spiralis: inducible expression of a novel goblet cell lectin, intelectin-2, and its natural deletion in C57BL/10 mice. *J Immunol*. 2004;173:1894-1901.
60. Cunliffe RN, Rose FR, Keyte J, Abberley L, Chan WC, Mahida YR. Human defensin 5 is stored in precursor form in normal Paneth cells and is expressed by some villous epithelial cells and by metaplastic Paneth cells in the colon in inflammatory bowel disease. *Gut*. 2001;48:176-185.
61. Yang R, Lee M, Hu H, et al. Identification of omentin as a novel depot-specific adipokine in human adipose tissue: possible role in modulating insulin action. *Am J Physiol Endocrinol Metabol*. 2006;290(6):E1253-E1261. doi:10.1152/ajpendo.00572.2004
62. Au-Yeung CL, Yeung TL, Achreja A, et al. ITLN1 modulates invasive potential and metabolic reprogramming of ovarian cancer cells in omental microenvironment. *Nat Commun*. 2020;11:3546.
63. Artis D. New weapons in the war on worms: identification of putative mechanisms of immune-mediated expulsion of gastrointestinal nematodes. *Int J Parasitol*. 2006;36:723-733.
64. Tsuji S, Yamashita M, Nishiyama A, et al. Differential structure and activity between human and mouse intelectin-1: human intelectin-1 is a disulfide-linked trimer, whereas mouse homologue is a monomer. *Glycobiology*. 2007;17:1045-1051.
65. Wesener DA, Dugan A, Kiessling LL. Recognition of microbial glycans by soluble human lectins. *Curr Opin Struct Biol*. 2017;44:168-178.
66. Wangkanont K, Wesener DA, Vidani JA, Kiessling LL, Forest KT. Structures of Xenopus embryonic epidermal lectin reveal a conserved mechanism of microbial glycan recognition. *J Biol Chem*. 2016;291:5596-5610.
67. Ghosh D, Porter E, Shen B, et al. Paneth cell trypsin is the processing enzyme for human defensin-5. *Nat Immunol*. 2002;3:583-590.

SUPPORTING INFORMATION

Additional supporting information may be found in the online version of the article at the publisher's website.

How to cite this article: Nonnecke EB, Castillo PA, Johansson MEV, et al. Human intelectin-2 (ITLN2) is selectively expressed by secretory Paneth cells. *FASEB J*. 2022;36:e22200. doi:10.1096/fj.202101870R